

FNAL PROPOSAL No. 512

Scientific Spokesman:

Paul F. Shepard  
Department of Physics and Astronomy  
University of Pittsburgh  
Pittsburgh, Pa. 15260  
Phone: (412) 624-4327

THE INCLUSIVE PRODUCTION OF CHARGED HYPERONS BY PIONS

W. E. Cleland, W. E. Cooper, E. Engels, P. F. Shepard, and J. Thompson  
Department of Physics and Astronomy, University of Pittsburgh  
Pittsburgh, Pennsylvania 15260

October 1976

## THE INCLUSIVE PRODUCTION OF CHARGED HYPERONS BY PIONS

W. E. Cleland, W. E. Cooper, E. Engels, P. F. Shepard<sup>†</sup>, and J. Thompson  
Department of Physics and Astronomy, University of Pittsburgh  
Pittsburgh, Pennsylvania 15260

### Summary

We propose to measure the cross section for the inclusive production of  $\left\{ \begin{array}{l} \Sigma^- \\ \Xi^- \end{array} \right\}$ , and  $\left\{ \begin{array}{l} \Xi^- \\ \Xi^- \end{array} \right\}$  hyperons by  $\pi^\pm$  mesons in the reaction  $\pi^\pm + \text{nucleon} \rightarrow \text{hyperon} + M_x$  at incident beam energies in the vicinity of 200 GeV. The eight possible reactions will be studied as a function of the variables  $s, t$ , and  $M_x^2$ . An analysis of the data using triple-Regge theory will yield the trajectory  $\alpha(t)$  of the exchanged Reggeon for  $t$  values  $-5 \text{ GeV}^2 \leq t \leq 0 \text{ GeV}^2$ . Four of the eight reactions are exotic, while the remainder presumably involve  $\Sigma^*$  or  $\Xi^*$  exchange. A measurement of  $\alpha(0)$  and  $\alpha'(0)$  for the exotic reactions consistent with triple-Regge results for non-exotic exchanges would lend support for the existence of exotics, and may yield definite experimental predictions for the possible masses and spins of exotic baryons to be searched for as  $s$ -channel resonances. The polarization of the charged hyperons will also be measured. It is estimated that the experiment will require 300 hours of beam for testing and 500 hours for data taking, making a total request of 800 hours.

---

<sup>†</sup> Correspondent

## I. Introduction

We propose an experiment to investigate the role of exotic and non-exotic exchange processes in the strong interactions by studying the inclusive production of the charged hyperons  $\Sigma^-$  and  $\Xi^-$  and their anti-particles using beams of  $\pi^+$  and  $\pi^-$  mesons. Including the four possible inclusive final states ( $\Sigma^-$ ,  $\Xi^-$ ,  $\overline{\Sigma^-}$ , and  $\overline{\Xi^-}$ ), and the two signs of the incident pion beam; there are a total of eight possible reactions. Within the context of a triple-Regge analysis of these reactions, the four reactions which involve a change in the sign of the charge between the incoming pion and the outgoing hyperon are exotic, while the remaining four reactions are not. The experiment thus provides a direct comparison between both exotic and non-exotic production mechanisms utilizing the same beam particles and highly similar decay topologies for the inclusive final state.

## II. Physics Justification

The physics goals of the experiment are justified within the framework of the triple-Regge theory of inclusive reactions. In detail the eight reactions are

- 1)  $\pi^- + \text{Nucleon} \rightarrow \Sigma^- + M_X$
- 2)  $\pi^+ + \text{Nucleon} \rightarrow \Sigma^- + M_X$
- 3)  $\pi^- + \text{Nucleon} \rightarrow \overline{\Sigma^-} + M_X$
- 4)  $\pi^+ + \text{Nucleon} \rightarrow \overline{\Sigma^-} + M_X$
- 5)  $\pi^- + \text{Nucleon} \rightarrow \Xi^- + M_X$
- 6)  $\pi^+ + \text{Nucleon} \rightarrow \Xi^- + M_X$
- 7)  $\pi^- + \text{Nucleon} \rightarrow \overline{\Xi^-} + M_X$
- 8)  $\pi^+ + \text{Nucleon} \rightarrow \overline{\Xi^-} + M_X$

where  $M_X$  is the missing mass in the reactions.

Reactions 2,3,6, and 7 are exotic. If we characterize the reaction as shown by diagram 1,

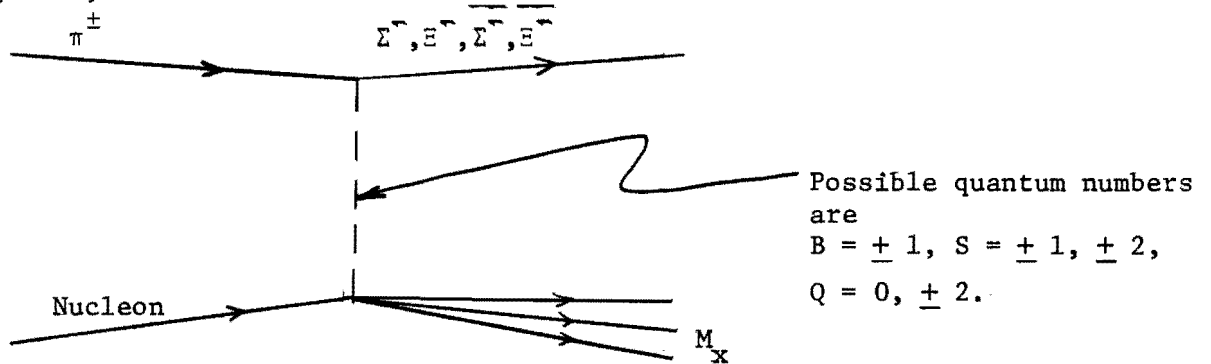


Diagram 1.

then all of the reactions involve baryon or antibaryon exchange. The exchanged object (if it is a single exchange) carries strangeness of  $\pm 1$  or  $\pm 2$  for final states involving  $\left\{ \begin{matrix} \Sigma \\ \Sigma \end{matrix} \right\}$ , and  $\left\{ \begin{matrix} \Xi \\ \Xi \end{matrix} \right\}$  respectively. For the exotic reactions the exchanged object carries charge  $\pm 2$ ; whereas, the charge is zero for the non-exotic channels. By exotic we mean a baryon which cannot be constructed from three quarks. The non-exotic reactions presumably involve the exchange of a  $\left\{ \begin{matrix} \Sigma^* \\ \Sigma^* \end{matrix} \right\}$ , and  $\left\{ \begin{matrix} \Xi^* \\ \Xi^* \end{matrix} \right\}$  for the  $\left\{ \begin{matrix} \Sigma \\ \Sigma \end{matrix} \right\}$ , and  $\left\{ \begin{matrix} \Xi \\ \Xi \end{matrix} \right\}$  final states.

We believe that a triple-Regge analysis of these reactions is justified for several reasons. Recent work in the neutral hyperon beam at Fermilab involving a study of the reaction  $p + \text{nucleon} \rightarrow \Lambda^0 + M_x$  has revealed that  $\Lambda^0$  production is consistent with a mechanism mediated by Reggeized  $K^*$  exchange.<sup>1</sup> The same experiment shows that single-Reggeon exchange involving a  $\Sigma$  trajectory is also indicated for the  $K_S^0$  inclusive production data, and that single-Reggeon exchange is not inconsistent with  $\Lambda^0$  production. In the case of  $\Lambda^0$  production this is a striking result because here single-Reggeon exchange must be exotic. Furthermore, our recent work in the

hyperon beam at the AGS indicates that the inclusive production of  $\Lambda^0$  from nuclear targets by a beam of  $\Sigma^-$ 's is consistent with a triple-Regge analysis involving pion exchange.<sup>2</sup>

To apply triple-Regge theory to the inclusive production of  $\left\{ \begin{matrix} \Sigma^- \\ \bar{\Sigma}^- \end{matrix} \right\}$ , and  $\left\{ \begin{matrix} \Xi^- \\ \bar{\Xi}^- \end{matrix} \right\}$  studied as a function of  $s, t$ , and  $M_x^2$ ; it is necessary to compare the measured invariant cross section  $s \frac{d^2\sigma}{dt dM_x^2}$  with a form determined from the triple-Regge diagram shown below.

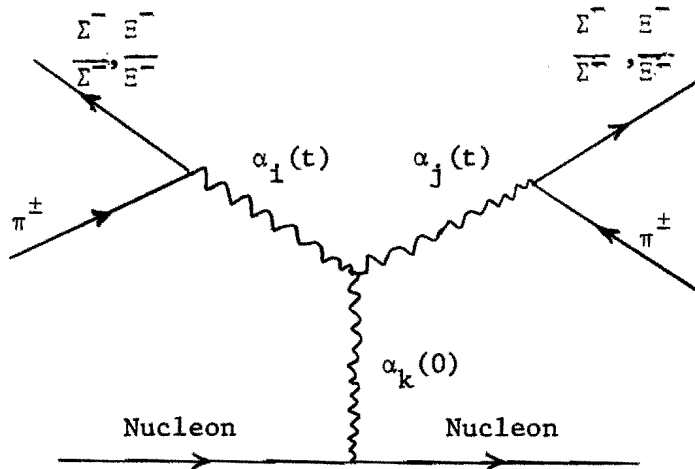


Diagram 2.

The form of the cross section corresponding to diagram 2 is given by<sup>3</sup>

$$(9) \quad s \frac{d^2\sigma}{dt dM_x^2} = \frac{1}{s} \sum_{ijk} G_{ijk}(t) \left(\frac{\nu}{s}\right)^{-\alpha_i(t)-\alpha_j(t)} (\nu)^{\alpha_k(0)}$$

where  $G_{ijk}$  is the triple-Regge term, and  $\nu = M_x^2 - t - M_{\text{nucleon}}^2$ . If this process is governed by single-Reggeon exchange, then  $\alpha_i(t) = \alpha_j(t)$  are the trajectories of the exchanged baryon or antibaryon shown in diagram 1 and carries the appropriate quantum numbers, which in the cases where  $Q = \pm 2$  is exotic. If  $\alpha_k(0)$  is the Pomeron, which is expected to dominate, then

Fermilab neutral hyperon beam. If the  $\Xi^-$  particles are observed to be polarized, one would then consider designing an experiment to measure the magnetic moment of the  $\Xi^-$ . We are proposing an essentially symmetric detection apparatus (the calorimeter would have to be moved during the experiment) for detecting hyperons, and this design feature together with the capability of reversing the  $\vec{B}$  field of the spectrometer magnet will provide a method for determining systematic effects in a polarization measurement. Given the known values for the  $\alpha$  parameters for the  $\Sigma^-$  and  $\Xi^-$  decays (-0.07 and -0.39, respectively), a sample of 10,000  $\Sigma^-$  and  $\Xi^-$  decays would enable us to measure  $P_{\Xi^-}$  to a statistical accuracy of  $\pm 0.04$  and  $P_{\Sigma^-}$  to an accuracy of  $\pm 0.2$ .

Finally, we are not insensitive to the existence of other components of the incident beam, namely,  $p, \bar{p}$ , and  $K^\pm$ . Consistent with the other goals of the experiment and the available running time, we would, concurrently with the pion running, acquire some data on the inclusive production of hyperons by these other components of the incident beam.

### III. Triple-Regge Theory and the Kinematics of Hyperon Production

The equation

$$(11) \quad s \frac{d^2 \sigma}{dt dM_x^2} = G(t) \left(\frac{\nu}{s}\right)^{1-2\alpha(t)}$$

can be expected to describe the data in a region of small  $|t|$  for large  $s$  and  $M_x^2$  with  $\frac{\nu}{s} \ll 1$ , which we have taken to be  $M_x^2 > 10 \text{ GeV}^2$ , and  $\frac{\nu}{s} < 0.5$ . The eight reactions will be studied over a range of hyperon production angles from 0 to 14 mrad for hyperon momenta between 100 GeV/c and 200 GeV/c. For

an incident pion beam momentum of 200 GeV/c the  $t$  range is  $-5 \text{ GeV}^2 \leq t \leq 0 \text{ GeV}^2$ .

In estimating expected rates for the non-exotic channels we have assumed  $G(t) = \text{constant} = 4 \text{ mb/GeV}^2$  based on the neutral hyperon production data from E-8 and also by scaling  $\Lambda^0$  inclusive production by pions at 18.5 GeV.<sup>1,4</sup> These two estimates are consistent within a factor of two. For the non-exotic channels we have assumed  $\Sigma^-$  and  $\Xi^-$  production to be dominated by the  $\Sigma^*$  and  $\Xi^*$  trajectories in the  $3/2^+$  decuplet. A consideration of Chew-Frautschi plots of baryon systematics<sup>5</sup> gives

$$(12) \quad \Sigma^*(3/2^+) : \alpha(t) = -0.25 + 0.9t$$

$$(13) \quad \Xi^*(3/2^+) : \alpha(t) = -0.65 + 0.9t$$

Figure 1 shows a plot of  $\frac{\nu}{s}$  versus the  $\Sigma^-$  laboratory production angle for contours of fixed  $t$  and constant  $s \frac{d^2\sigma}{dt dM_x^2}$ .  $\Xi^-$  kinematics are very similar. The intersection of the contours of fixed  $t$  and constant  $s \frac{d^2\sigma}{dt dM_x^2}$  represent a matrix of points. Measurements of the invariant cross section at these points yield data from which the trajectory  $\alpha(t)$  of equation (10) may be determined. Specifically, measurements of  $s \frac{d^2\sigma}{dt dM_x^2}$  at the contour intersections along a line of fixed  $t$  should (according to triple-Regge theory) fall at equal spacings on a straight line when plotted as  $\log(s \frac{d^2\sigma}{dt dM_x^2})$  versus  $\log(\frac{\nu}{s})$ . The slope of this line is  $1-2\alpha(t)$  for that  $t$  value. The matrix of possible data points covers a range of laboratory angles between 0 and 14 mrad, and laboratory momenta between 100 GeV/c and 200 GeV/c. Accurate measurements of  $\alpha(t)$  can be obtained by measuring the production cross section over two or more orders of magnitude at fixed  $t$ .

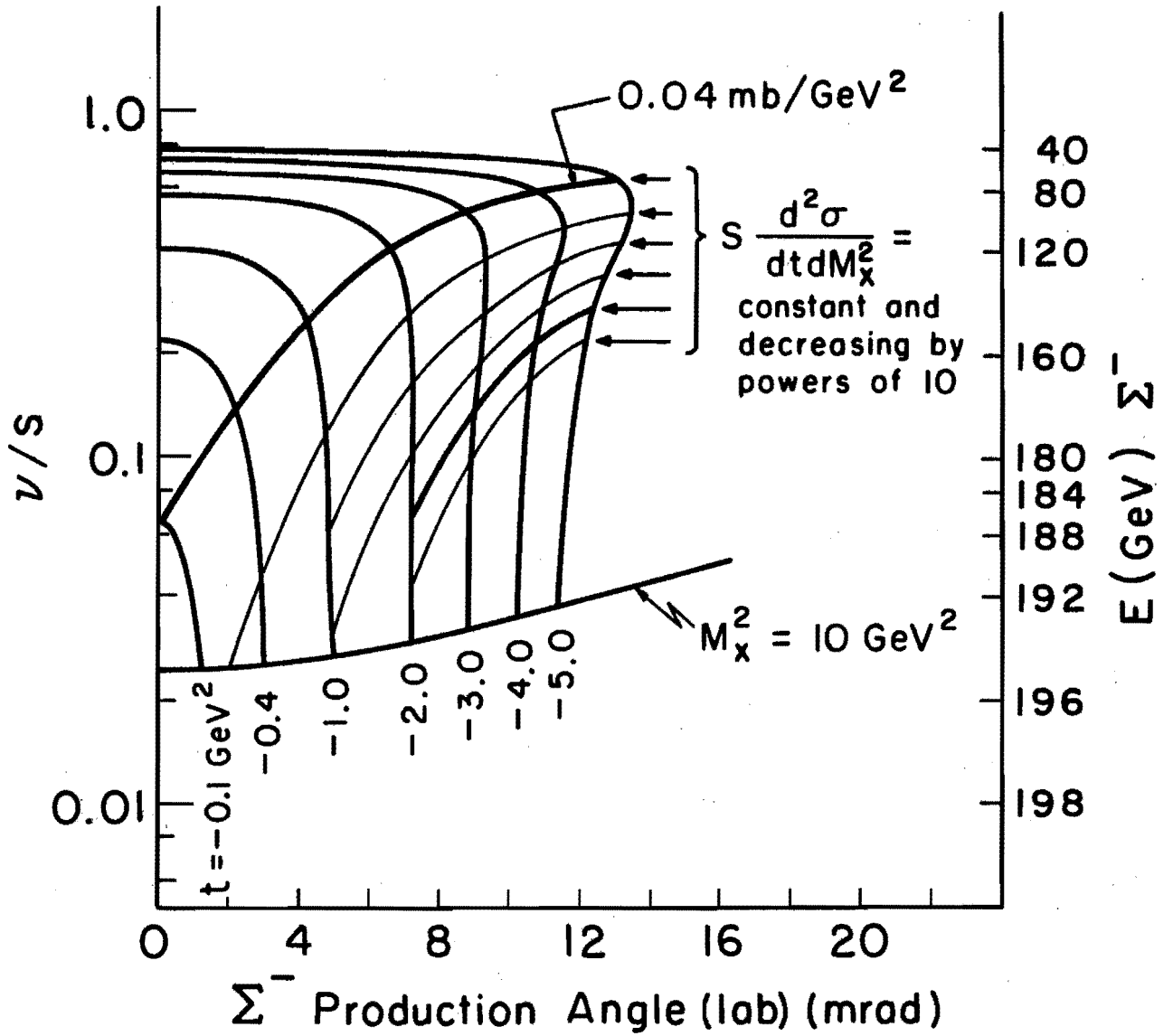
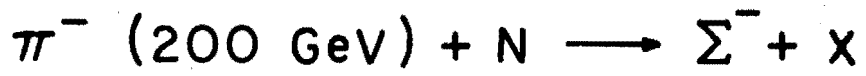


Figure 1



#### IV. Experimental Setup

The experimental setup consists of two parts: (1) The arrangements for targeting the incident pion beam coupled with the momentum analysis of the recoiling hyperon; (2) the spectrometer for detecting and identifying the hyperons through their decay topologies.

##### A. Beam Targeting and Hyperon Channel

Figure 2 shows the apparatus required for targeting the pion beam. The beam passes through a quadrupole pair which focuses the beam at the target location. After passing through the quadrupole pair, the beam is deflected by a dipole of field integral equal to 6 kg-meters and enters the B-1 dipole nearly parallel to and offset from the beam line. The B-1 dipole then steers the beam onto the Be target at any angle ranging from 0° to +14 milliradians. The high pressure proportional wire chambers shown on the figure establish the orbit of each beam particle so that its incident direction and position at the target are known to an angular precision of 0.02 milliradians and 0.8 millimeters, respectively.

The hyperon momentum analyzing channel consists of two 5-1.5-120 EPB dipoles as shown in figure 3. The  $\Delta p/p$  and  $\Delta\Omega$  for this configuration are equal to 4.1% and  $7.7 \times 10^{-6}$  steradians, respectively. The position and angle of the hyperon trajectory emerging from the channel is determined by a high pressure PWC immediately downstream of the channel. This information, along with our knowledge of the incident pion trajectory, enables us to determine the momentum of a single hyperon to approximately + 1.0%.

### BEAM TARGETING ARRANGEMENT

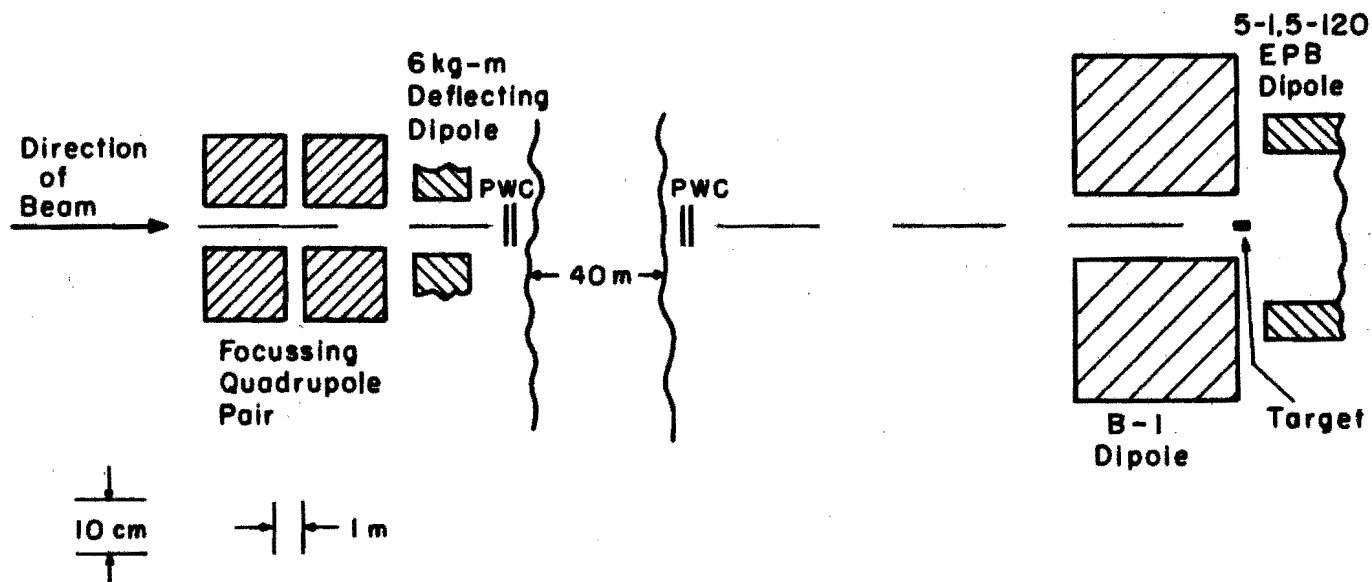


Figure 2

### HYPERON MOMENTUM ANALYZING CHANNEL

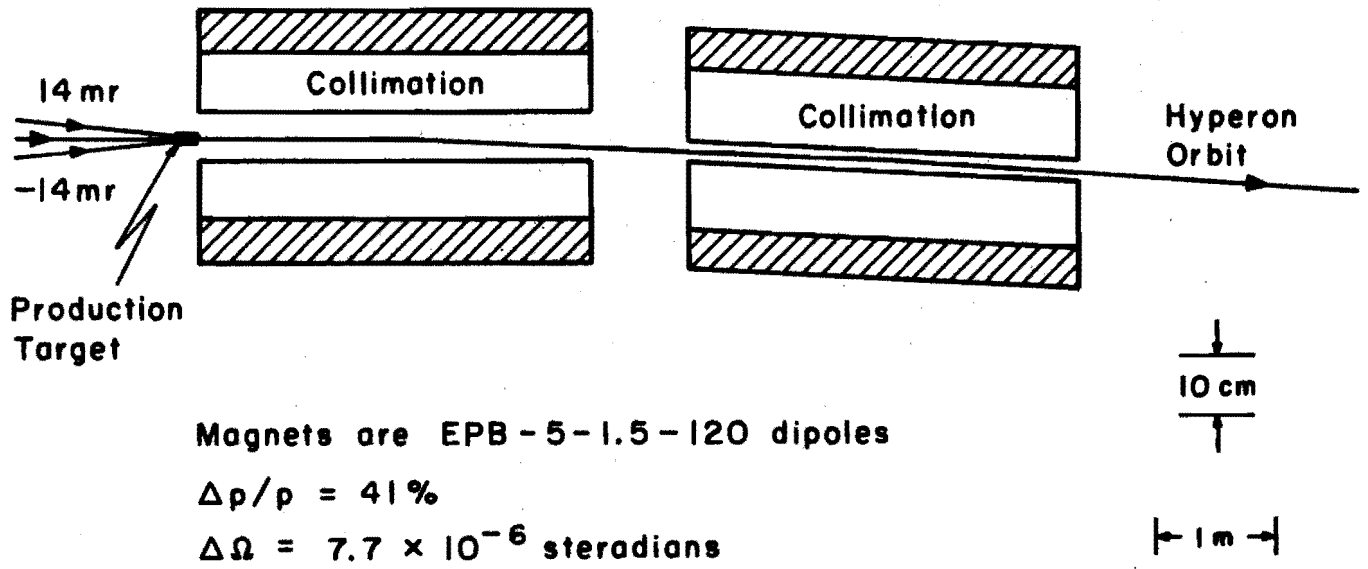


Figure 3

## B. Hyperon Spectrometer

The hyperon spectrometer beginning at the downstream aperture of the hyperon channel is shown in figure 4. A cluster of high resolution proportional wire chambers (PWC's) is located at the end of the hyperon channel to tag the incident hyperon trajectories. This is followed by a 10 m decay region. Two BM109's instrumented with PWC's provides information on the decay angles and momenta of the charged decay products. The final element in the apparatus is a hadron calorimeter of  $\sim 3$  interaction lengths to detect the final neutron or proton from the hyperon decay.

The apparatus trigger is designed to detect the following decays:

$$(14) \quad \Sigma^- \rightarrow \pi^- + n$$

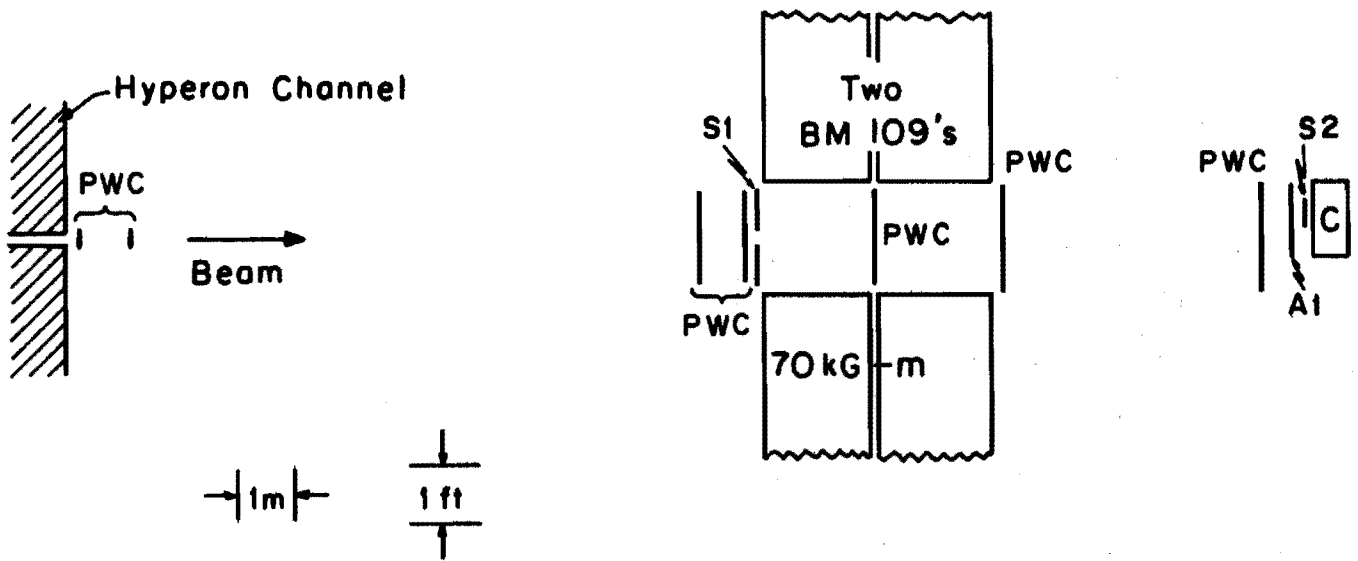
$$(15) \quad \Sigma^- \rightarrow \pi^- + \Lambda^0$$

$\downarrow$   
 $\rightarrow \pi^- + p$  ,

or the corresponding antiparticle decays.

A thin scintillator (S1) with a hole to accommodate the beam and the forward going baryon will be located in front of the magnet to detect the  $\pi^-$  from  $\Sigma^-$  and  $\Sigma^+$  decays. An anticoincidence counter (A1) in front of the calorimeter plus the signal from the calorimeter (C) will give a positive identification for the neutron from  $\Sigma^-$  decay. The proton from either  $\Sigma^-$  will also register in the calorimeter and will be further identified by a scintillator (S2) appropriately placed in front of it. The flux emerging from the channel will be counted by the initial set of PWC's (B). If necessary, a further strengthening of the trigger can be accomplished by incorporating the

### Schematic of Proposed Apparatus (Plan View)



PWC = Proportional Wire Chamber  
A1, S1, S2 = Scintillation Counters  
C = Calorimeter

Figure 4

the information from the PWC's before and after the BM109's into the trigger. The final trigger will be an "OR" of the  $\Sigma^-$  and  $\Xi^-$  triggers:

$$(16) \quad \Sigma^- \text{ trigger} = B \cdot S1 \cdot \overline{A1} \cdot C$$

$$(17) \quad \Xi^- \text{ trigger} = B \cdot S1 \cdot S2 \cdot C$$

## VI. Rates and Running Time

Based on the suppositions of triple-Regge theory as discussed in section III, we have calculated the hyperon flux at the exit of the channel for the non-exotic exchanges. Table 1 shows the number of hyperons appearing at the exit of the channel for 10 hours of beam with 14 seconds between pulses, and  $5 \times 10^6$  pions/pulse onto a 10 cm Be target. For the momentum range 100 GeV/c to 200 GeV/c between 10% and 30% of the hyperons produced within the momentum bite and solid angle of the channel survive their passage through the channel's 7.2 m length.

The fraction which decay in the 10 m drift region after the channel, and are detected, is shown in Table II.

In order to study all eight reactions from section II we would require  $\sim 500$  hours of beam time plus 300 hours of tuning, making a total request of 800 hours. We have assumed  $5 \times 10^6$   $\pi^+$ 's/pulse and 257 pulses/hour. The experiment is well suited to the Meson laboratory and to the M-1 beam line in particular. The recent E-61<sup>6</sup> running in M-1 indicates that the beam can probably be nursed to this incident pion flux. However, the experiment could be done in other Meson lab beams provided the necessary intensity is available.

Table I

Numbers of  $\Sigma^-$  and  $\Xi^-$  (non-exotic production) at the exit of the hyperon channel/10 hours of beam with 14 seconds between pulses, and  $5 \times 10^6$  pions/pulse onto a 10 cm Be target.

$t = -0.4 \text{ GeV}^2$			$t = -1.0 \text{ GeV}^2$		
$\frac{v}{s}$	$\Sigma^-$	$\Xi^-$	$\frac{v}{s}$	$\Sigma^-$	$\Xi^-$
.13	$2.8 \times 10^4$	$5.5 \times 10^3$	.25	$1.7 \times 10^4$	$5.4 \times 10^3$
.045	$3.7 \times 10^3$	$3.2 \times 10^2$	.12	$2.9 \times 10^3$	$5.5 \times 10^2$
			.062	$3.6 \times 10^2$	$3.8 \times 10^1$

$t = -2.0 \text{ GeV}^2$			$t = -5.0 \text{ GeV}^2$		
$\frac{v}{s}$	$\Sigma^-$	$\Xi^-$	$\frac{v}{s}$	$\Sigma^-$	$\Xi^-$
.4	$7.7 \times 10^3$	$3.6 \times 10^3$	.65	$3.0 \times 10^2$	$2.1 \times 10^2$
.26	$1.7 \times 10^3$	$5.5 \times 10^2$	.42	$7.2 \times 10^1$	$3.6 \times 10^1$
.16	$2.6 \times 10^2$	$5.9 \times 10^1$			

Table II

Fraction of hyperons which both decay and are detected by the spectrometer.

$p(\text{GeV}/c)$	$\Sigma^-$	$\Xi^-$
100	.93	.57
150	.83	.37
200	.74	.25

## VII. Background

In the proposed experiment we are triggering on hyperon decay topologies. The background will consist mainly of pions or protons emerging from the channel and interacting in material upstream of the spectrometer magnet, a claim that can be supported by our AGS experience. In the AGS beam our background triggers for  $\Xi^-$  were entirely consistent with the pion flux interacting with 2 cm. of lucite associated with scintillation counters and plastic Cerenkov counter mirrors. Since we estimate fewer than  $10^4$  pions and protons emerging from the channel compared with numbers considerably larger than this at the AGS, we foresee no serious trigger rate problems.

## VIII. Requirement of Fermilab and Time Schedule

We have designed the experiment around existing laboratory magnets. We request that the laboratory supply two BM109's, two EPB magnets, a B-1 main ring dipole, a small steering magnet (6 kg-m), standard fast electronics, and the necessary shielding for the channel. We would plan to construct the remainder of the apparatus. It is our expectation that we could be ready to begin installation of the apparatus at Fermilab in one year.



REFERENCES

1. Thomas J. Devlin, Rutgers-Michigan-Wisconsin Collaboration, "Experiments in the FNAL Neutral Hyperon Beam," Invited talk presented at the Winter Meeting of the APS, Bulletin of the American Physical Society, 21, 93 (1976).
2. W. E. Cleland, "Inelastic Hyperon-Induced Interactions," Talk presented at the XIth Rencontre de Moriond, Flaine, France, March 1976.
3. R. D. Field and G. C. Fox, Nuclear Physics B80, 367 (1974).
4. U. Nauenberg et al., FNAL P-360.
5. N. P. Samios et al., Reviews of Modern Physics 46, 49 (1974).
6. P. Koehler, private communication.

FIGURE CAPTIONS

- Fig. 1.  $v/s$  versus the  $\Sigma^-$  laboratory production angle ( $\theta$ ) in the reaction  $\pi^- + \text{nucleon} \rightarrow \Sigma^- + M_x$  for contours of fixed  $t$  and constant invariant cross sections ( $s \frac{d^2\sigma}{dt dM_x^2}$ ). The cross section contours are decreasing in powers of 10.  $\Sigma^-$  kinematics are similar.
- Fig. 2. The targeting of the incident pion beam onto a 10 cm Be target. High pressure PWC's will measure the target position and angle of the incoming pion. A variable production angle between  $\pm 14$  mrad is accomplished with a small upstream steering magnet to produce the necessary offset and a B-1 main ring dipole to steer the beam onto the target at the desired angle.
- Fig. 3. The hyperon momentum analyzing channel consists of two type 5-1.5-120 EPB magnets which produce a total bend of 13.5 mrad. The overall length is 7.2 m,  $\frac{\Delta p}{p} = 41\%$ , and  $\Delta\Omega = 7.7 \times 10^{-6}$  steradians.
- Fig. 4. The hyperon spectrometer which will detect the charged hyperons emerging from the channel on the basis of their decay topologies in a 10 drift region.